

# Synthesis, Characterization, and Catalytic Performance of Cr-Incorporated Aluminoborate Octahedral Molecular Sieves

Wenliang Gao, Tao Yang, Yingxia Wang, Guobao Li, Fuhui Liao, and Jianhua Lin\*

State Key laboratory for Rare Earth Materials Chemistry and Applications, College of Chemistry and Molecular Engineering, Peking University, Beijing 100871, P. R. China

Received: July 19, 2005; In Final Form: October 13, 2005

A series of Cr-incorporated PKU-1 molecular sieves (Cr-PKU-1) were synthesized by using boric acid as a flux, and the physicochemical properties were characterized by XRD, ICP, SEM, XPS, UV-vis, and NH<sub>3</sub>-TPD methods. The morphology of Cr-PKU-1 is a needlelike hexagonal prism with uniform size of about 2  $\mu\text{m}$  in diameter and 20–50  $\mu\text{m}$  in length. XRD and UV-vis provide direct evidence that Cr ions have been successfully incorporated into the framework of PKU-1. NH<sub>3</sub>-TPD shows a dramatic increase of acidic sites in the Cr-PKU-1 in comparison with PKU-1, indicating that the Cr incorporation can significantly modify the acidity of the compound. In addition, the incorporated Cr ions may act as redox centers, thus catalytic performance of Cr-PKU-1 molecular sieve was investigated by the selective oxidation of styrene under mild reaction conditions.

## 1. Introduction

Cr-incorporated zeolite-type materials, such as silicates, aluminosilicates, aluminophosphates, and silicoaluminophosphates, have been studied as catalysts for redox reactions. For instance, CrAPO-5 was used as a catalyst for the selective oxidation from 1-butan-2-ol to butadiene,<sup>1</sup> 2-methyl-3-butyn-2-ol to 3-methyl-3-buten-1-yne,<sup>2</sup> and cyclohexane to cyclohexanone,<sup>3</sup> as well as for selective decomposition of cyclohexenylhydroperoxide to 2-cyclohexen-1-one.<sup>4</sup> To find high-efficient redox catalysts, considerable attempts have been focused on incorporation of multivalent transition metal ions into microporous framework materials.<sup>5</sup> However, as far as the structural properties are concerned, such as ionic radius, ionic charge, and coordination preference, transition metal ions are quite different from those main group elements in zeolite materials. Therefore, the isomorphous incorporation of transition metal ions into zeolite materials is quite difficult.<sup>6</sup> Among the molecular sieves mentioned above, most of them have either not given evidence for the framework substitution or concluded that chromium ion is not located in framework positions. It has been reported<sup>7</sup> that Cr ions can be incorporated into the framework of AlPO<sub>4</sub>-5 under modified reaction conditions. However, the experimental evidence showed that the Cr ion is located in a distorted octahedron, which bonds to four framework oxygen atoms and two additional water molecules. Owing to the strong preference for octahedral coordination, the substitution of transition metal ions into zeolite frameworks may cause significant distortion of the framework structure, which may consequently reduce the stability of the materials.

An alternative strategy for incorporating the transition metal ions is to use the octahedral molecular sieves (OMS). Octahedral frameworks are common for the condensed inorganic materials but rare for the porous inorganic materials. The Todorokite family is a well-known octahedral molecular sieve, in which the rock salt blocks of manganese oxides are linked forming

one-dimensional tunnels via a rutile-type connection. These materials demonstrated promising performance for the oxidation reactions of alcohol<sup>9</sup> and indene.<sup>10</sup> Recently, another series octahedral molecular sieves of aluminoborates (PKU-1 and PKU-5) were identified.<sup>8</sup> The framework of PKU-1<sup>8a</sup> consists of edge-sharing Al-octahedra that form 18- and 10-ring windows (Figure 1). The borate groups (BO<sub>3</sub> and B<sub>2</sub>O<sub>5</sub>) are attached on the surface of the octahedral framework to compensate for the negative charge. The large 18-ring windows (BET: 340 m<sup>2</sup>/g) and octahedral coordination of the framework atoms make this material an attractive candidate of host material for Cr incorporation and redox catalyst. In this study, we report the synthesis and physicochemical properties of the Cr-incorporated PKU-1. A considerable amount of Cr can be incorporated into the framework of PKU-1 by direct synthesis reactions in the boric acid flux as confirmed by significant change of lattice parameters and UV-vis absorption. The Cr-incorporated PKU-1 also shows a significant increase of acidity and improved catalytic performance for a selective oxidation of styrene under mild reaction conditions.

## 2. Experimental Section

**Synthesis of Cr-PKU-1.** Cr-PKU-1 was synthesized by using boric acid as the flux without using any organic template as described in previous reports.<sup>11</sup> For a typical reaction, H<sub>3</sub>BO<sub>3</sub> (100 mmol), Al(NO<sub>3</sub>)<sub>3</sub> (4 mmol), and Cr(NO<sub>3</sub>)<sub>3</sub> (0, 0.2, 0.5, 0.8, and 1.0 mmol) were ground and loaded into a 100 mL Teflon autoclave, then the mixture was heated at 240 °C for 5 days. After the mixture was cooled to room temperature, the solid was washed with hot water (70 °C) until the residual boric acid was completely removed. The content of Cr substitution was determined by using the ICP method. The as-synthesized Cr-PKU-1 samples were denoted as PKU-1a, PKU-1b, PKU-1c, PKU-1d, and PKU-1e according to the increase of the loaded Cr.

**Characterizations of Cr-PKU-1.** Powder X-ray diffraction data were collected at room temperature on a Rigaku D/MAX 2000 diffractometer with Cu K $\alpha$  radiation. Tube voltage and

\* To whom correspondence should be addressed. E-mail: jhlin@pku.edu.cn. Phone: (+86) 10-6275-1715. Fax: (+86) 10-6275-1708.

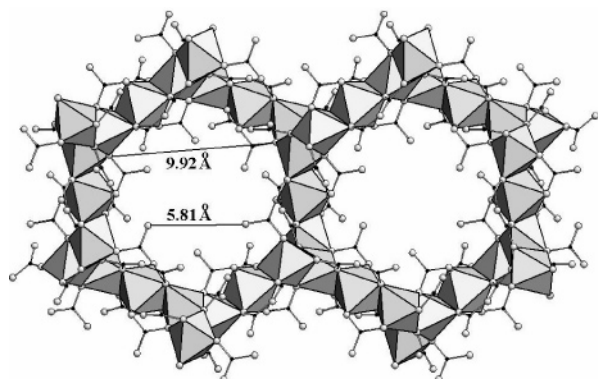


**Figure 1.** Projection of the Cr-PKU-1 structure along the *c*-axis;  $\text{AlO}_6$  and  $\text{CrO}_6$  octahedra are shown as polyhedra and oxygen and boron atoms as light and dark spheres.

current were 40 kV and 100 mA. The lattice parameters and unit cell volumes of the Cr-PKU-1 samples were calculated with the TEROR 90 program.<sup>12</sup> Morphology of the samples was examined with a field emission scanning electron microscopy (SEM, Amray 1910 FE). The UV-vis spectra were recorded on a Shimadzu, UV-3100 spectrophotometer with  $\text{BaCO}_3$  as a reference. The XPS spectra were acquired with a UK Kratos Axis Ultra spectrometer with  $\text{Al K}\alpha$  X-ray source operated at 15 kV, 15 mA. The pressure in the chamber was less than  $5.0 \times 10^{-9}$  Torr. Electron binding energies were calibrated against the C 1s emission at  $E_b = 284.8$  eV. The compositions of the Cr-PKU-1 samples were analyzed with inductively coupled plasma-atomic emission spectroscopy (ICP-AES, ESCALAB 2000).

**Catalytic Test of Cr-PKU-1.**  $\text{NH}_3$  temperature-programmed desorption ( $\text{NH}_3$ -TPD) was employed to study the acidic properties of Cr-PKU-1 with a Micromeritics TPD/TPR 2900 chemical adsorptive instrument. The sample was positioned into a quartz tube and enclosed with quartz wool plugs.  $\text{NH}_3$  gas was pulse-injected sufficiently into the sample chamber with a syringe at room temperature, and then the chamber was purged with He gas for 180 min at 100 °C to remove physically adsorbed  $\text{NH}_3$  gas. At the end, the temperature was increased from 100 °C up to 580 °C at 10 deg/min to remove chemisorbed  $\text{NH}_3$  gas. The amount of desorbed  $\text{NH}_3$  was determined with acidic titration methods. The epoxidation of styrene was performed in a 50 mL glass reactor and stirred with a magnetic stirrer. In a standard run, 10 mmol of styrene, 10 mL of acetone as solvent, 10 mmol of  $\text{H}_2\text{O}_2$  (30% aqueous solution), and 50 mg of catalyst were mixed in the reactor. After the reaction had proceeded for 5 h at 60 °C, the products were taken from the reaction system, centrifuged to remove the suspending catalyst, and then analyzed by gas chromatography (GC-3800, Varian, using Flame Ionization Detector) with a flexible quartz capillary column.

### 3. Results and Discussion

The as-synthesized Cr-PKU-1 samples have a needlelike hexagonal prismatic morphology of about 2  $\mu\text{m}$  in diameter and

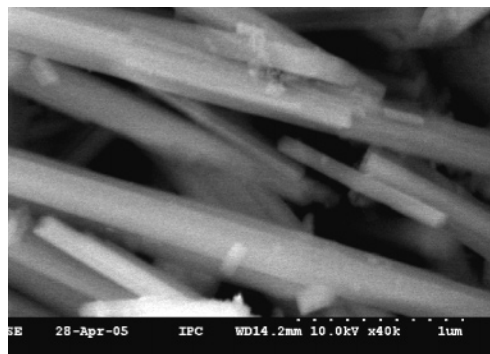


**Figure 2.** SEM micrograph of the PKU-1b sample.

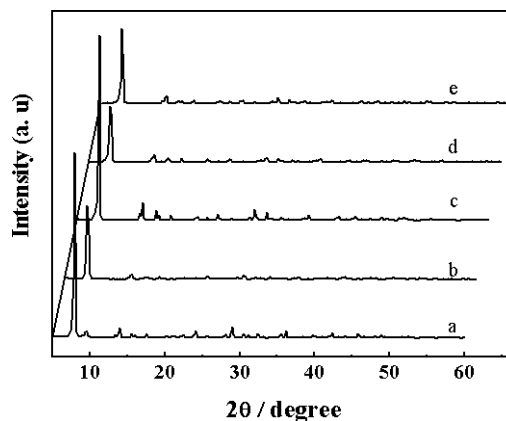


**Figure 3.** X-ray diffraction patterns for (a) PKU-1a, (b) PKU-1b, (c) PKU-1c, (d) PKU-1d, and (e) PKU-1e.

20–50  $\mu\text{m}$  in length (Figure 2) with a deep green color. The chemical analysis by using ICP-AES indicate the loaded chromium in the starting materials was not completely incorporated in the products (Table 1), but shows a linear correlation with the incorporated Cr content. The obtained maximum content of Cr in the Cr-PKU-1 samples is about 7.69% (atom ratio:  $\text{Cr}/(\text{Cr}+\text{Al})$ ), which is higher than the other known Cr-incorporated systems.<sup>6a</sup> Figure 3 shows the powder X-ray diffraction (XRD) patterns of this Cr-PKU-1 series. The XRD patterns of the Cr-incorporated PKU-1 are identical with that of the PKU-1,<sup>8</sup> indicating that the octahedral porous framework structure was formed for the Cr-PKU-1 series.

Figure 4 shows the dependence of the unit cell parameters on the content of incorporated Cr in the Cr-PKU-1 samples. It can be seen that the unit cell volume and the *a*-axis increase almost linearly with the incorporated Cr content; the variation of the *c*-axis is relatively small (not shown in the figure). A similar result was observed in other metal-incorporated systems.<sup>13</sup> The expansion of the unit cell parameters is consistent with the larger ionic radius of  $\text{Cr}^{3+}$  (0.615 Å) than  $\text{Al}^{3+}$  (0.535 Å).<sup>15</sup> The Cr-PKU-1 system can be considered as a solid solution formed by substitution of Al by Cr in PKU-1. Since the synthesis reactions were performed in the flux of boric acid, the incorporated content of Cr is not quantitatively the same as that of the loaded content. Additionally, purely Cr-incorporated

**TABLE 1: Composition of the Loaded and Obtained Samples of the Cr-PKU-1 Series**

sample	composition in the starting materials			analytical results for as-synthesized samples		
	Cr (atom %)	Al (atom %)	Cr:Al	Cr (atom %)	Al (atom %)	Cr:Al
PKU-1a	0	100	0:1	0	100	0:1
PKU-1b	4.76	95.24	1:20	1.32	98.68	1:75
PKU-1c	11.11	88.89	1:8	4.17	95.83	1:23
PKU-1d	16.70	83.30	1:5	4.76	95.24	1:20
PKU-1e	20.00	80.00	1:4	7.69	92.31	1:12

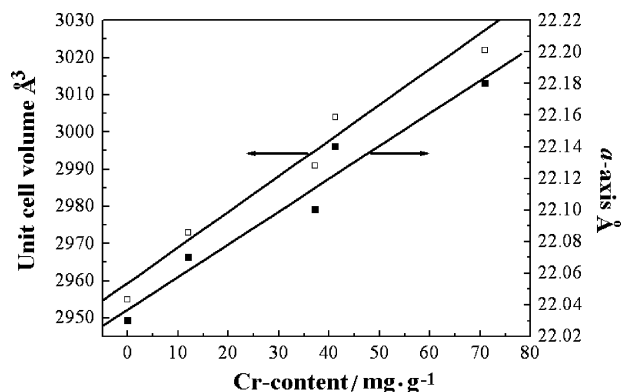


Figure 4. Cell volume and *a* parameters for the Cr-PKU-1 system.

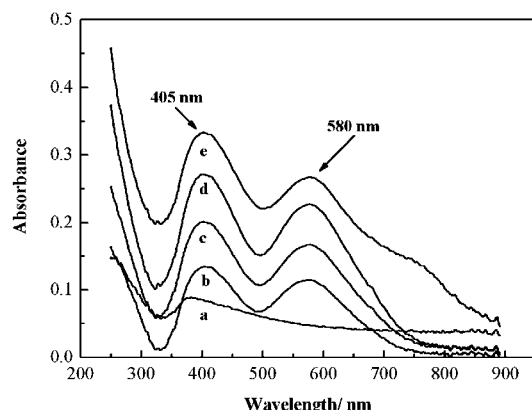


Figure 5. UV-vis spectra of (a) PKU-1a, (b) PKU-1b, (c) PKU-1c, (d) PKU-1d, and (e) PKU-1e.

PKU-1 cannot be formed under present reaction conditions. Therefore, we have not yet determined exactly the up-limit boundary of the solid solution. Nevertheless, the significant change of the cell parameters definitely confirms the success of Cr incorporation into the PKU-1 frameworks. It is worthy mentioning that in some tetrahedral molecular sieve systems, due to the low incorporation content, the variation of the unit cell parameters is too small to definitely verify the incorporation of transition metal ions into the framework.<sup>14</sup>

UV-visible absorption spectra of the Cr-PKU-1 samples are shown in Figure 5. All samples exhibit two characteristic absorption bands at about 405 and 580 nm except undoped PKU-1a. The two absorption bands can be attributed to transitions within the  $d^3$  configuration for an octahedrally coordinated  $\text{Cr}^{3+}$  ion.<sup>16</sup> The absorption band at 405 nm can be assigned to the  ${}^4\text{A}_{2g} \rightarrow {}^4\text{T}_{1g}$  transition, while the 580 nm absorption band may originate from the  ${}^4\text{A}_{2g} \rightarrow {}^4\text{T}_{2g}$  transition. It is well-known that  $\text{Cr}_2\text{O}_3$  has characteristic absorption at about 445, 630, and 663 nm. The absence of these absorption bands in Cr-PKU-1 samples implies no  $\text{Cr}_2\text{O}_3$  impurity in the product. Furthermore, it can be seen that the intensity of the absorption bands increases almost continuously with the increase of the Cr content, which further confirms the success of Cr incorporation into the framework of PKU-1.

Chromium ions may exist in different oxidation states in solid materials. In some molecular sieves, high oxidation state chromium ions ( $\text{Cr}^{5+}$  or  $\text{Cr}^{6+}$ ) were identified.<sup>17</sup> The chromium ions in different oxidation states may exhibit different catalytic properties. Figure 6 shows the photoelectron spectra (XPS) of Cr 2p and O 1s for an as-synthesized and a calcined sample of PKU-1b. For the as-synthesized sample, two characteristic binding energies of Cr ions are located at 587.6 ( $2p_{1/2}$ ) and 577.8 eV ( $2p_{3/2}$ ). These values agree reasonably well with that of

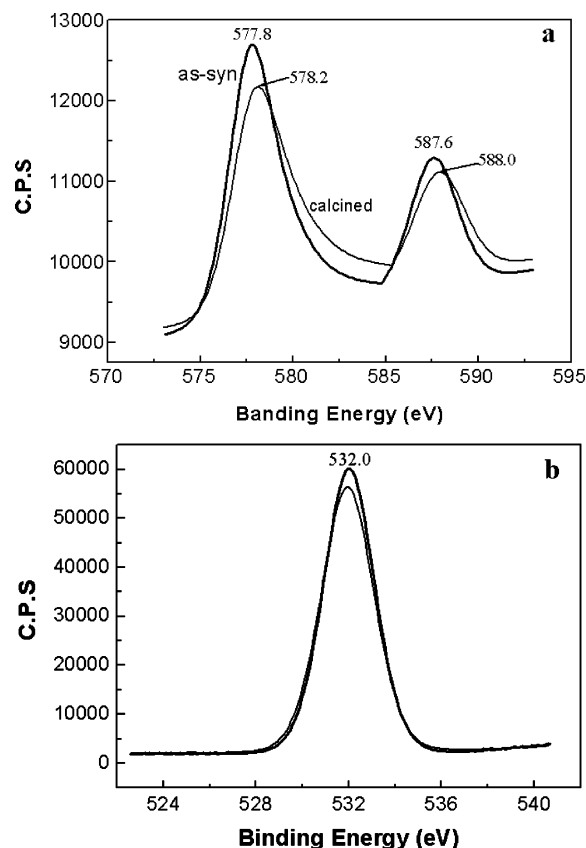
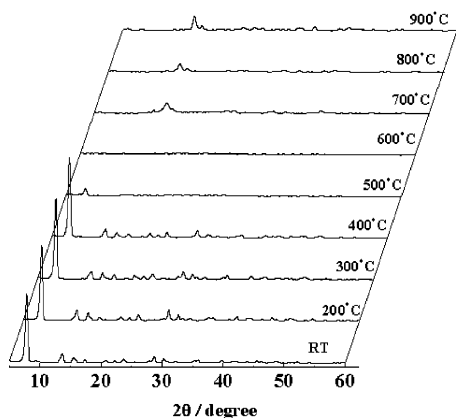


Figure 6. XPS spectra of (a) Cr 2p and (b) O 1s for the as-synthesized and calcined PKU-1b (400 °C).

$\text{Cr}(\text{NO}_3)_3$  (587.0 ( $2p_{1/2}$ ) and 577.3 eV ( $2p_{3/2}$ )).<sup>18</sup> The slight discrepancy (about 0.5 eV) may originate from different chemical environments or systematic errors of the measurements. For the catalytic applications, the molecular sieves normally need pretreatment at certain temperatures to remove the adsorbed species in channels. In Figure 6, we also included the XPS spectra of PKU-1b after heating at 400 °C for 4 h. The binding energy of the O 1s (532.0 eV) is almost unchanged after the heating treatment as shown in Figure 6b,<sup>19</sup> while the binding energy of chromium species moves slightly to higher energy, 588.0 ( $2p_{1/2}$ ) and 578.2 eV ( $2p_{3/2}$ ), after the heating treatment. Although the variation is rather small (0.4 eV), since the measurements were carried out under the same conditions, the systematic deviation of the measurements can be eliminated. The shift of the binding energy may, therefore, originate from partial oxidation of Cr ions to a high oxidation state.

Thermal and hydrothermal stabilities of the molecular sieves are important for catalytic applications since many reactions may proceed under rigorous conditions. To examine the thermal stability, a PKU-1b sample was heated respectively at 200, 300, 400, 500, 600, 700, 800, and 900 °C in air, and the powder X-ray diffraction patterns were recorded accordingly after each calcination (Figure 7). It can be seen that the crystallinity of Cr-PKU-1 samples does not change below 400 °C, which means the octahedral framework is retained at this temperature. At 500 °C, the crystallinity of samples decreases dramatically. At about 600 °C, the framework completely collapses and transforms to an amorphous phase. A further increase in the temperature (900 °C) leads to formation of another crystalline aluminoborate (PKU-5).<sup>8b</sup> The hydrothermal stability of Cr-PKU-1 was also studied because, in many cases, the hydrothermal treatment may result in dealumination from the framework, which influences the catalytic activity of the materials. To test the hydrothermal



**Figure 7.** XRD patterns of the PKU-1b sample after heating at different temperatures in air.

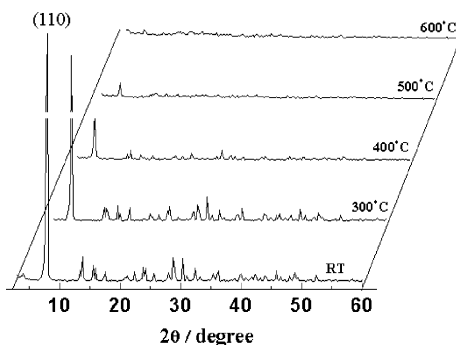


**Figure 8.** XRD patterns of PKU-1b sample after heating treatment at different temperatures in a water steam.

**TABLE 2: Total Acid Amounts of Cr-PKU-1 Sample Determined by the NH<sub>3</sub>-TPD Method**

sample	PKU-1a	PKU-1b	PKU-1d	PKU-1e
total acid amount (mmol/g)	0.172	0.535	0.926	1.016

stability, the Cr-PKU-1 sample in a quartz tube was heated at various temperatures in water-saturated steam, and in the meantime the XRD patterns were recorded after each treatment. As shown in Figure 7, the hydrothermal stability of Cr-PKU-1 is lower than the thermal stability. The reflection (110) is characteristic for the 18-ring windows of the octahedral framework in PKU-1. It can be seen that the intensity of this reflection decreases significantly after treatment at 400 °C in the water steam, but sustained in air. The thermal and hydrothermal stability of Cr-PKU-1 is moderate among the microporous materials, which, however, can only be used below 400 °C.

Temperature-programmed desorption (TPD) experiments, with NH<sub>3</sub> as a probe, were carried out for Cr-PKU-1 to monitor the change of acidity on the Cr incorporation. Figure 9 shows the NH<sub>3</sub>-TPD curves for the Cr-PKU-1 samples. In general, the temperature of the NH<sub>3</sub> desorption is related to the strength of acidity, while the area of the NH<sub>3</sub> desorption bands corresponds to the quantity of the acidic sites. From Figure 9 one can see that a significant change occurs for the acidic site

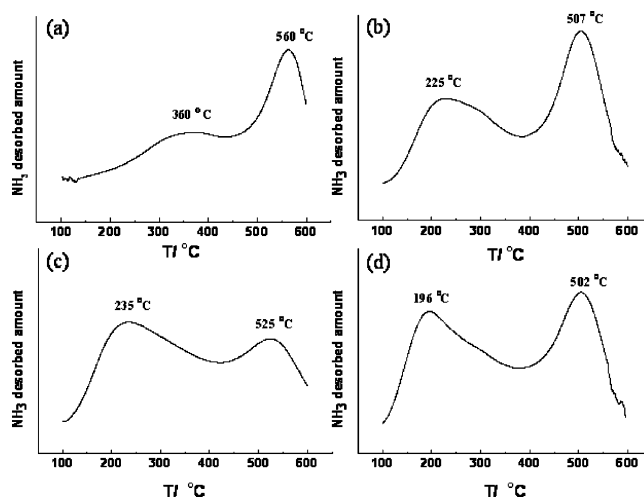


**Figure 9.** NH<sub>3</sub>-TPD thermogram curves for (a) PKU-1a, (b) PKU-1b, (c) PKU-1d, and (d) PKU-1e.

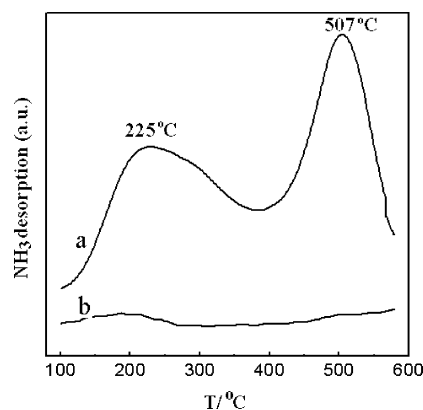


**Figure 10.** NH<sub>3</sub>-TPD curves of PKU-1b: (a) as-synthesized and (b) calcinated at 600 °C for 2 h.

by Cr incorporation. Table 2 shows the change of total acidic centers in the Cr-PKU-1 series. The dramatic increase of the quantity of the acidic centers with the increase of Cr content suggests that the Cr incorporation indeed creates more acidic sites in the PKU-1 framework. Additionally, the TDP curves of the Cr-PKU-1 samples all consist of two overlapped ammonia desorption bands. According to refs 20 and 21, the high-temperature (HT) band may relate to desorption of the ammonia bound to stronger Brönsted and Lewis acid sites.<sup>20</sup> The low-temperature (LT) band can be assigned to the ammonia that coordinated to weak Lewis acid forming NH<sub>4</sub><sup>+</sup> ions.<sup>21</sup> In comparison with the undoped sample (PKU-1a), both HT and LT desorption bands shift to lower temperature for the Cr-incorporated samples. Figure 10 compares the TPD curves of an as-synthesized PKU-1b sample and a sample after hearing treatment at 600 °C. We knew that the octahedral framework collapses and transforms to an amorphous phase at 600 °C. Consequently, the desorption bands at 225 and 507 °C of the as-synthesized sample disappear after the thermal treatment. This observation confirms that the acidic centers are mostly located

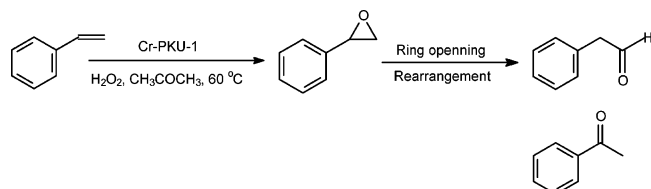
**TABLE 3: Epoxidation of Styrene over (Cr-)PKU-1 Catalysts<sup>a</sup>**

catalyst	TON <sup>b</sup> (mmol h <sup>-1</sup> g <sup>-1</sup> )	conv (%)	products selectivity (mole %)			
			styrene epoxide	phenylacetaldehyde	hypnone	others
PKU-1a	3.15	9.45	2.50	70.32	none	27.18
PKU-1b	17.90	53.66	40.20	22.01	1.68	36.11

<sup>a</sup> Solvent: acetone, 10 mL; styrene, 10 mmol; H<sub>2</sub>O<sub>2</sub>, 10 mmol; time, 6 h; temperature, 60 °C; catalyst weight, 50 mg. <sup>b</sup> TON: millimoles of styrene converted per gram of catalyst per hour.



## SCHEME 1: The Mechanism of Oxidation of Styrene



on the internal surface of the framework instead of corresponding to amorphous or other chromium impurity phases.

It is known that styrene can be oxidized to phenylacetaldehyde and hypnone under mild reaction conditions, whereas the speculated product due to epoxidation of styrene was not easily produced.<sup>22</sup> In fact, phenylacetaldehyde and hypnone can be considered as the products of the rearranging reaction of epoxide catalyzed in strong acidic environment (Scheme 1). To improve selectivity of the rearranging reactions, styrene epoxidation should be performed over the catalysts with suitable acidic capacity and strength. Table 3 summarizes the results of oxidation of styrene with use of H<sub>2</sub>O<sub>2</sub> (30 wt %) as oxidizing agent over the Cr-PKU-1 catalyst under mild reaction conditions. The Cr-PKU-1 catalyst shows significant catalytic activity (conversion 53.66%) and styrene epoxide selectivity (40.20%) in comparison with the PKU-1 catalyst (conversion 9.45%; selectivity 2.50%). The significant improvement of the catalytic performance may originate from the active acidic centers created by Cr incorporation in the framework as indicated by the NH<sub>3</sub>-TPD measurements. The main drawback of this catalyst is the byproducts produced in the reaction, i.e., phenylacetaldehyde and a polymerization product. These byproducts were produced mainly due to over-oxidation effects resulting in ring opening and structure rearrangement of styrene oxide. Consequently, adjusting the acidity of catalysts is the crucial step to improve the selectivity in the epoxidation reaction of styrene.

## 4. Conclusions

In summary, we have demonstrated that Cr ions can be incorporated into the aluminoborate (Cr-PKU-1) that has a porous octahedral framework. The syntheses of the Cr-incorporated PKU-1 can be realized directly by reactions in the boric acid flux. At present, the highest realized Cr content is about 7.69% (in Cr/(Cr+Al)), which is significantly higher than that for other zeolite-type systems. The incorporated Cr ions enhance the acidity of the materials, which, in turn, improve the performance for the epoxidation reaction of styrene. The success of incorporating the transition metal ions in PKU-1 provides an alternative way of looking for the redox catalysts. Although the purely octahedral frameworks are rare, there are many known octahedral/tetrahedral framework compounds which could be considered as candidates for substitution of transition metal ions. A problem that is common for these frameworks is the low thermal stability. The PKU-*n* series of compounds show moderate thermal stability, but considerable decomposition was often observed during the catalytic reactions. Therefore, great effort is still needed in looking for more stable octahedral framework compounds and improving their catalytic performance.

**Acknowledgment.** The authors thank the financial support from NSFC (20221101) and the State Key Basic Research Program of China and Prof. Bingxiong Lin and Dr. Bin Li for TPD measurement.

## References and Notes

- (1) Escalante, D.; Giraldo, L.; Pinto, M.; Pfaff, C.; Ram' rez de Agudelo, M. M. *J. Catal.* **1997**, *169*, 176.
- (2) Gabriela, Z.; Emmanuelle, S.; Jan, K. *J. Catal.* **2002**, *208*, 270.
- (3) Lempers, H. E. B.; Chen, J. D.; Sheldon, R. A. *Stud. Surf. Sci. Catal.* **1995**, *94*, 705.
- (4) Sheldon, R. A.; Chen, J. D.; Dakka, J.; Neeleman, E. *Stud. Surf. Sci. Catal.* **1994**, *83*, 407.
- (5) (a) Mihai P.; Josanlet C. V.; Suib, S. L. *J. Am. Chem. Soc.* **2004**, *126*, 7774. (b) Sung, H. J.; Jong-San, C.; Ji, W. Y.; Jean-Marc, G.; Anthony K. C. *Chem. Mater.* **2004**, *16*, 5552. (c) Martin, H.; Larry, K. *Chem. Rev.* **1999**, *99*, 635–663. (d) Robert, R.; Gopinathan, S.; John, M. T. *Chem. Commun.* **1999**, 829.
- (6) (a) Hartmann, M.; Kevan, L. *Chem. Rev.* **1999**, *99*, 635. (b) Isabel, W. C. E. A.; Roger, A. S.; Martin, W.; Schuchardt, U. *Angew. Chem., Int. Ed. Engl.* **1997**, *36*, 1144. (c) David, M. E. *Nature* **2002**, *417*, 813. (d) Thomas, J. M.; Raja, R.; Sankar, G.; Bell, R. G. *Acc. Chem. Chem.* **2001**, *34* 191.
- (7) (a) Kornatowski, J.; Zadrozna, G.; Wloch, J.; Rozwadowski, M. *Langmuir* **1999**, *15*, 5863. (b) Padlyak, B.; Kornatowski, J.; Zadrozna, G.; Rozwadowski, M.; Gutsze, A. *J. Phys. Chem. A* **2000**, *104*, 11837. (c) Kornatowski, J.; Zadrozna, G.; Rozwadowski, M.; Zibrowius, B.; Marlow, F.; Lercher, J. A. *Chem. Mater.* **2001**, *13*, 4447.
- (8) (a) Ju, J.; Lin, J.; Li, G.; Yang, T.; Li, H.; Liao, F.; Chun-K, L.; You, L. *Angew. Chem., Int. Ed.* **2003**, *42*, 5607. (b) Ju, J.; Yang, T.; Li, G. B.; Liao, F. H.; Wang, Y. X.; You, L. P.; Lin, J. H. *Chem. Eur. J.* **2004**, *10*, 3901.
- (9) Young-C. S.; Vinit, D. M.; Amy, R. H.; Suib, S. L. *Angew. Chem., Int. Ed.* **2001**, *40*, 4280.
- (10) Kinda, A. M.; Kate, L.; Young-C. S.; Suib, S. L. *Chem. Mater.* **2004**, *16*, 4296.
- (11) Lu, P. C.; Wang, Y. X.; Lin, J. H.; You, L. P. *Chem. Commun.* **2001**, 1178–1179.
- (12) Cheng, D. J. *Appl. Crystallogr.* **1999**, *32*, 838.
- (13) (a) Blasco, T.; Concepci6n, P.; Nieto, J. M.; Prez-Pariente, J. J. *Catal.* **1995**, *152*, 1. (b) Lamberti, C.; Bordiga, S.; Zecchina, A.; Artioli, G.; Marra, G.; Spano, G. *J. Am. Chem. Soc.* **2001**, *123*, 2204. (c) Palin, L.; Lamberti, C. *J. Phys. Chem. B* **2003**, *107*, 4034.
- (14) (a) Sung, H. J.; Jong-S. C.; Young, K. H.; Jean-M. G.; Anthony, K. C. *J. Phys. Chem. B* **2005**, *109*, 845. (b) Canesson, L.; Tuel, A. *Zeolites* **1997**, *18*, 260.
- (15) Shannon, R. *Acta Crystallogr.* **1976**, *A32*, 751.
- (16) (a) Weckhuysen, B. M.; Schoonheydt, R. A. *Zeolites* **1994**, *14*, 360. (b) Weckhuysen, B. M.; Schoonheydt, R. A. *Stud. Surf. Sci. Catal.* **1994**, *84*, 965. (c) Lever, A. B. P. *Inorganic Electronic Spectroscopy*; Elsevier: Amsterdam, The Netherlands, 1984. (d) Bakac, A.; Wang, W.-D. *Inorg. Chim. Acta* **2000**, *297*, 27. (e) Krumpolc, M.; DeBoer, B. G.; Roek, J. J. *Am. Chem. Soc.* **1978**, *100*, 145.
- (17) (a) Bohdan, V. P.; Jan, K.; Gabriela, Z.; Michal, R.; Aleksander, G. *J. Phys. Chem. B* **2000**, *104*, 11837. (b) Escalante, D.; Giraldo, L.; Pinto, M.; Pfaff, C.; Ram' rez de Agudelo, M. M. *J. Catal.* **1997**, *169*, 176.
- (18) Desimoni, E.; Malitesta, C.; Zambonin, P. G.; Riviere, J. C. *Surf. Interface Anal.* **1988**, *13*, 173.
- (19) Katayama, A. *J. Phys. Chem.* **1980**, *84*, 376.
- (20) Karge, H. G.; Pfeifer, H.; Fricke, R. *Stud. Surf. Sci. Catal.* **1991**, *65*, 133.
- (21) Katada, N.; Igi, H.; Kim, J.-H.; Niwa, M. *J. Phys. Chem., B* **1997**, *101*, 5969.
- (22) (a) Meng, X. J.; Li, D. F.; Yang, X. Y.; Yu, Y.; Wu, S.; Han, Y.; Yang, Q.; Jiang, D. J.; Xiao, F. S. *J. Phys. Chem. B* **2003**, *107*, 8972. (b) Wang, Y.; Zhang, Q. H.; Tetsuya, S.; Katsuomi, T. *J. Catal.* **2002**, *209*, 186.